

Formation of Metallic Ultrafine Particles in Silica Glass by Ion Implantation

Kohei Fukumi, Akiyoshi Chayahara, Kohei Kadono, Hiroyuki Kageyama, Naoyuki Kitamura, Hiroshi Mizoguchi, Yuji Horino and Masaki Makihara

Osaka National Research Institute, AIST
1-8-31, Midorigaoka, Ikeda, Osaka, 563-8577 Japan
Tel: +(81)-727-51-9647
Fax: +(81)-727-51-9627

(Received: 2 February 1998; accepted: 9 March 1998)

Abstract

Formation of elemental ultrafine particles in silica glass has been discussed. The transport process of implanted ions in matrix glass during ion implantation is an important factor for the formation of the particles. In addition, the formation of particles of a gold-copper alloy has been studied. Competition between the collision process and precipitation process determines the resultant particle size.

I. Introduction

Glasses doped with semiconductor or metal ultrafine particles show high refractive index,¹⁾ optical nonlinearity,²⁾ and light emission,³⁾ and are attractive candidates for utilization in optical devices. For the production of these glasses, it is required to disperse a large amount of ultrafine particles in glasses. An ion implantation method is suitable for this purpose, since this method is free from solubility restrictions. In addition, this method has many advantages for the production of optical devices, owing to the easy controllability of ion beam position⁴⁾ and the exact controllability of dopant concentration. In order to synthesize the glasses dispersed with ultrafine particles by ion implantation, it is important to study the formation process of particles and to study the structure of particles. In this paper, the formation of elemental and metallic alloy ultrafine particles in silica glass has been discussed.

II. Formation of ultrafine particles

Formation of elemental ultrafine particles such as Au,⁵⁾ Ag,⁶⁾ Cu,⁷⁾ etc. has been observed in oxide glasses. As to the formation of elemental ultrafine particles in silica glass, Hosono et al.⁸⁾ has proposed a simple criterion; ultrafine particle formation occurs when the free energy of oxide formation of implants is greater than that of silica at 3000K. It has been shown, however, that the particles are not formed at low local concentration. For example, Perez et al. have shown that implanted iron atoms are mainly in ionic states at low dose and

in metallic state at high dose.⁹⁾ In addition, it has been shown that implanted Cu atoms are in ionic state in silica glass implanted at a dose of 1×10^{17} ions/cm² and an acceleration energy of 2MeV,¹⁰⁾ although Cu ultrafine particles are formed in silica glass by 160 keV ion implantation at a dose less than 1×10^{17} ions/cm².⁷⁾ The increase in acceleration energy leads to an increase in the width of the concentration profile of implanted ions along the depth, that is, the decrease in average concentration of implanted ions. Figure 1

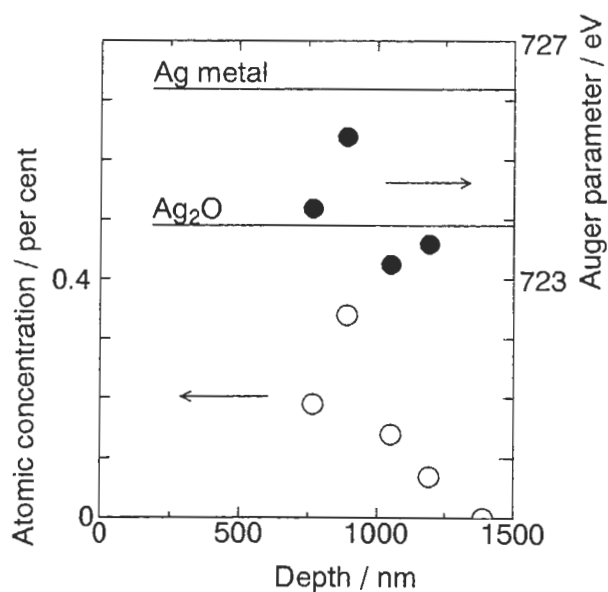


Fig.1 The depth profile of Ag atomic concentration and Auger parameter of Ag atoms in the 1.5MeV 1×10^{16} Ag⁺ ions/cm²-implanted silica glass.

shows the Auger parameter and concentration of silver atoms against depth obtained by the XPS measurement in 1.5MeV 1×10^{17} Ag⁺ions/cm²-implanted silica glass.¹¹⁾ This glass did not show the plasmon absorption due to Ag ultrafine metallic particles, although the absorption has been observed in the glass implanted with Ag⁺ ions at an acceleration energy of the order of 100keV.¹²⁾ Figure 1 indicates that the chemical state of implanted

Ag atoms depends on the local concentration in the glass. Therefore, it is deduced from these findings that the chemical state of implanted ions depends on the local concentration of implanted atoms.

The chemical shifts of AlK α X-rays in 200keV Al⁺-ion implanted silica glass and SiK α X-rays in 200keV Si⁺-ion implanted alumina¹³⁾ are shown in Fig.2. It can be seen that the chemical state of Si atoms in alumina depends

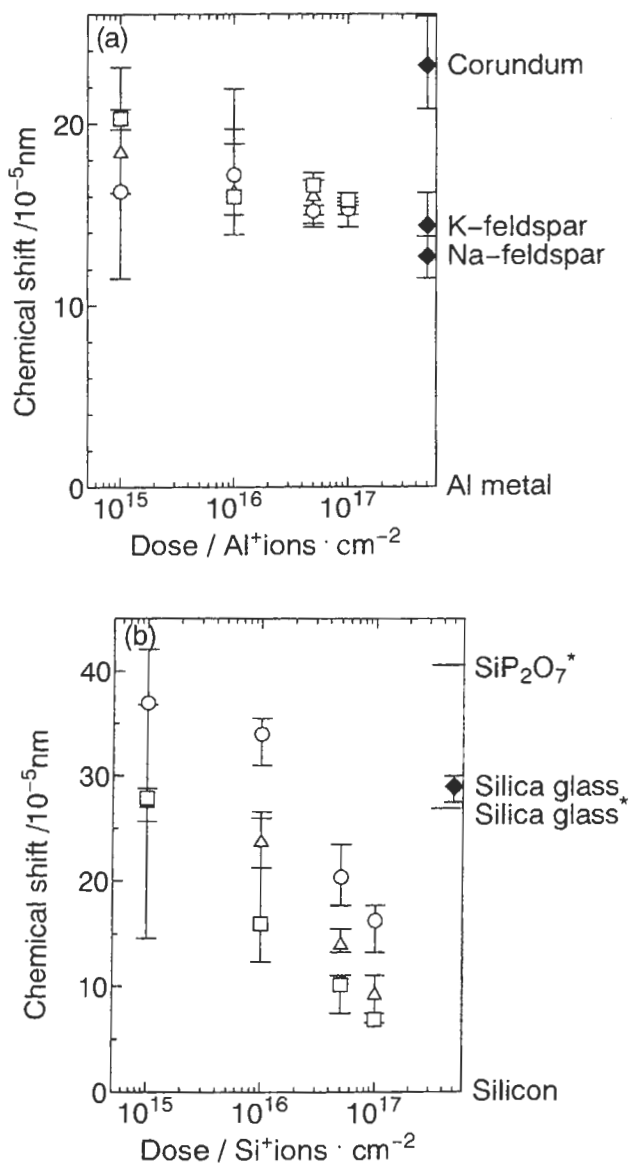


Fig.2 Chemical shifts of (a) Al K α X-rays in 200keV Al⁺-ion implanted silica glasses and (b) Si K α X-rays in 200 keV Si⁺-ion implanted alumina, before and after heat treatment. Circles, triangles and squares represent as-implanted samples, samples heated at 760°C and samples heated up to 920°C.

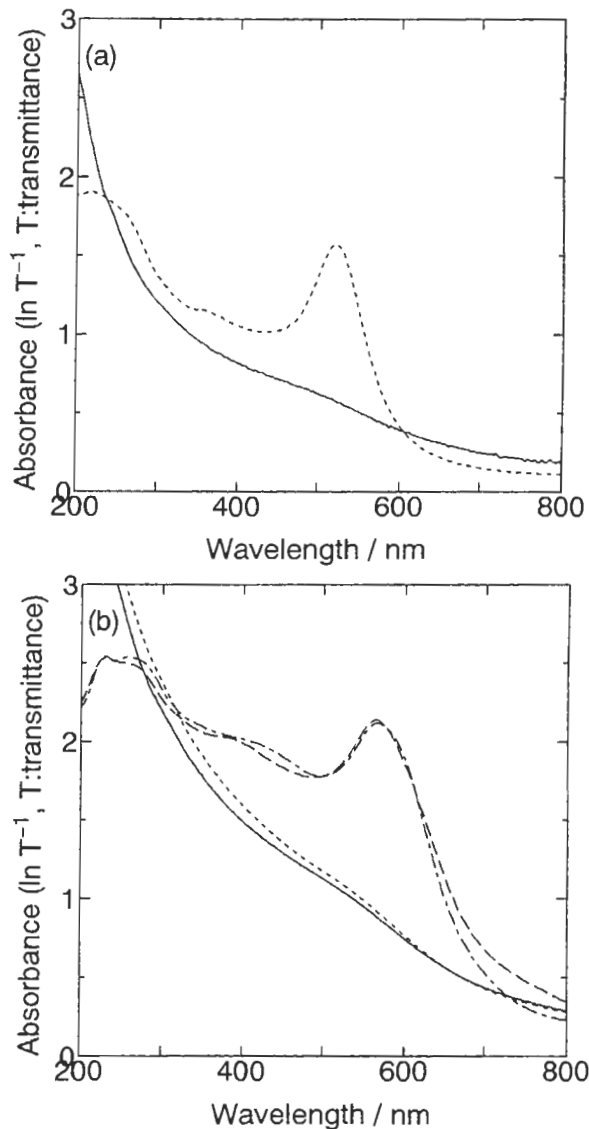


Fig.3 Optical absorption spectra of (a) Au⁺-ion implanted silica glasses and (b) (Cu⁺+Au⁺)-ions implanted silica glasses. Solid and dotted lines in (a) represent as-implanted glass and glass heated at 1000°C for 8h, respectively. Solid, dotted, dashed and dash-dotted lines in (b) represent glass with no heat-treatment, glass heat-treated only before Cu⁺-ion implantation, glass heat-treated only after Cu⁺-ion implantation and glass heat-treated before and after Cu⁺-ion implantation.

on the doses and the subsequent heat treatment in an argon gas atmosphere, while that of Al atoms in silica is independent of the doses and the heat treatment. From the viewpoint of formation energy, it is expected that Al atoms should form Al_2O_3 in the glass and Si atoms should form elemental silicon in alumina. The result of this experiment shows that the chemical state of implanted atoms is controlled by the transport process of implanted atoms, although the chemical state tends to obey the thermodynamic stability. Therefore, it is deduced that the dependence of particle formation on local concentration is due to the transport process of implanted atoms. As to the precipitation of crystals from solution, it is known that the nucleation rate is proportional to $\exp[-C/(\ln \alpha)^2]$, where α is the supersaturation ratio and C is the factor which depends on temperature and surface tension.¹⁴⁾ Furthermore, the growth rate is proportional to $(n_\infty(0)-n_1)/(n_0-n_1)$ and diffusion coefficient, where n_0 , n_1 and n_∞ represent the concentrations of the solute atoms in the precipitate, in the solution which is in equilibrium with the precipitate and in the solution far away from the precipitate, respectively.¹⁵⁾ Accordingly, the nucleation rate and the growth rate increase with an increase in the local concentration of implanted atoms. Therefore, ion implantation at high dose and low acceleration energy is suitable for the formation of metallic particles in silica glass.

III. Structure of gold particles in silica glass

Gold particles were formed in silica glasses implanted with 1.5MeV Au^+ ions, as depicted in the optical absorption spectra in Fig.3. Absorbance of a plasmon band at about 530nm due to Au ultrafine particles increases parabolically with an increase in doses from 1×10^{16} to 1×10^{17} ions/cm².¹⁶⁾ This is due to the increase in local concentration, as mentioned above. In the glass implanted with 1×10^{17} Au^+ ions/cm², Au atoms form gold ultrafine particles whose average coordination number is about 4, according to the extended x-ray absorption fine structure (EXAFS) spectroscopic measurements.¹⁷⁾ It is known that the interatomic distance between the nearest neighbors in ultrafine metallic particles decreases with decreasing particle size.¹⁸⁾ In the gold ultrafine particles within silica glass, the Au-Au bond distance is shorter than that in bulk gold by 0.05 Å. The reduction of the bond

length in the gold ultrafine particles within silica glass is less than that within a Mylar film in the previous study.¹⁸⁾ This difference is probably caused by the chemical interaction between gold atoms and matrix silica glass. In fact, it was found that the gold atoms form Au-O bonds at the surface of gold ultrafine particles.¹⁷⁾

Gold ultrafine particles grew after heat treatment, as shown in Fig.3. Since the growth rate is proportional to (heating time)^{1/3}, it is deduced that gold particles grow through the Ostwald ripening mechanism.²⁾ The well-grown particles in the glass after heating at 1000°C for 36h have an fcc structure as bulk gold, according to an x-ray diffraction study.¹⁹⁾ The coordination number and the bond length in the particles are the same as that in bulk gold, according to an EXAFS study.²⁰⁾ The particles are highly defective and include a few layers of plane faults, probably due to the mismatch of thermal expansion coefficient between gold particles and matrix silica glass.

IV. Formation of gold-copper alloys

Next to the formation of elemental ultrafine particles, it is interesting to form the ultrafine particles of compounds by the co-implantation technique. Since it is known that gold and

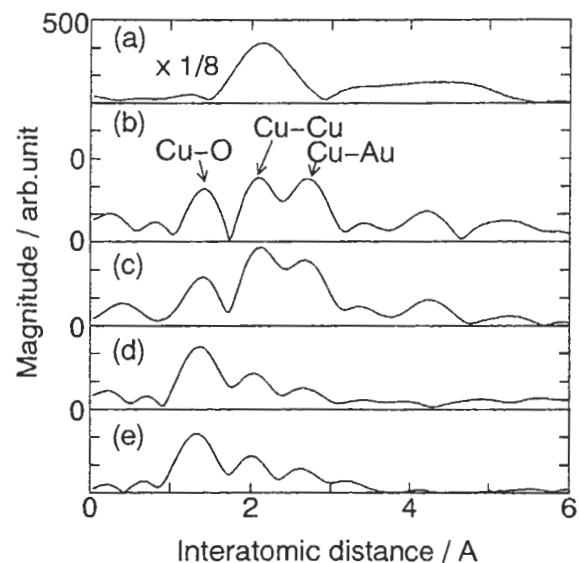


Fig.4 Magnitude of fourier-transform in the (Cu-Au)-ions implanted silica glass. (a); Cu metal, (b); glass heat-treated before and after Cu^+ -ion implantation, (c); glass heat-treated only after Cu^+ -ion implantation, (d); glass heat-treated only before Cu^+ -ion implantation, and (e); glass with no heat-treatment.

copper metals form gold-copper solid solution and gold-copper intermetallic compounds in all the compositional region, co-implantation of Au⁺ and Cu⁺ ions is a simple and good example for the formation of compounds in glass. The optical absorption spectra of 1x10¹⁷ 1.5MeVAu⁺ ions/cm²-implanted silica glass and 1x10¹⁷ 0.5MeVCu⁺ ions/cm² + 1x10¹⁷ 1.5MeVAu⁺ ions/cm²-implanted silica glass is shown in Fig.3. Au⁺ and Cu⁺ ions were located at 0.38μm and 0.34μm in depth with distribution widths of 0.16μm and 0.19μm, respectively, according to the TRIM code simulation. Although Au⁺-ion implanted glass followed by heat treatment at 1000°C for 8h in air showed a distinct absorption band at about 530 nm, the subsequent Cu⁺-ion implantation into this glass decreased the intensity of the band at 530 nm drastically. The absorption band at 530 nm in the co-implanted glass which was heat-treated before Cu⁺-ion implantation was as small as that in the co-implanted glass which was not heat-treated before Cu⁺-ion implantation.

Figure 4 shows the magnitude of fourier transform ($k=3.5-9 \text{ \AA}^{-1}$, k is the wavevector) of the k^3 -weighed EXAFS function of the glasses obtained from x-ray absorption spectra around the Cu K edge. This measurement was carried out by the fluorescence mode with a Lytle detector equipped with a Ni filter at room temperature at the Photon factory BL-12C. In addition, the x-ray absorption spectra were measured on Cu metal by the transmittance mode, for comparison. The k dependence of phase shifts and backscattering amplitude was ignored in the fourier-transformation. It can be seen that the implanted Cu atoms mainly form Cu-O bonds and scarcely form Cu-Cu or Cu-Au bonds in the Au⁺-ion implanted glasses followed by Cu⁺-ion implantation. This implies that the decrease in the absorption band at 530 nm by the subsequent Cu⁺-ion implantation in the heat-treated glass is not due to the formation of Cu-Au metallic alloy particles. Therefore, the decrease in the absorption band means a decrease in size of gold particles. It was deduced that the collision process partially destroys the well-grown Au ultrafine particles. On the other hand, the absorption band in the glass with no heat-treatment did not disappear by the subsequent Cu⁺-ion implantation. This implies that there is a counter-effect to the decrease in particle size. As mentioned above, the transport process plays an important role for

the formation of the particles during ion implantation. The counter-effect is enhancement of precipitation through the increase in total dose and the ion-beam heating. The particle size depends on the competition of these opposite effects during ion implantation.

The fourier-transform magnitude curves of the co-implanted glasses showed peaks due to Cu-Cu bonds and Cu-Au bonds after heating at 900°C for 30 min, indicating that the particles of Au-Cu metallic alloys are partially formed in the glass. The optical absorption spectra of the co-implanted glass after heating showed a broad band at about 565 nm. The peak wavelength of this band is longer by 45 nm than that of the band observed in the Au⁺-ion implanted glass followed by heat-treatment and is shorter by 5 nm than that of the band observed in the Cu⁺-ion-implanted glass followed by heat-treatment. This is due to the formation of alloy particles and the dissolution of Cu ions in silica glass, as explained below. The optical absorption coefficient of the plasmon peak is expressed by eq.(1)²¹⁾

$$\alpha = p \frac{\omega}{nc} |f_i|^2 \epsilon_m'' \quad (1),$$

$$f_i(\omega) = \frac{3\epsilon_d}{\epsilon_m(\omega) + 2\epsilon_d}$$

where $\epsilon_m(\omega) = \epsilon_m' + i\epsilon_m''$, complex and frequency dependent, is the dielectric constant of the metallic particles and ϵ_d , real, is that of matrix glass. The symbols α , p , ω , n , c , and f_i represent the absorption coefficient of the sample, the volume fraction of the particles, the angular frequency, the refractive index of the matrix glass, the velocity of light and the local field factor, respectively. Since eq.(1) shows that the plasmon band has a peak at $\epsilon_m' = -2\epsilon_d$, the peak wavelength of the band depends on the dielectric constants of the matrix and the particles. The real part of dielectric constant of the particles in the free-electron region is expressed by eq.(2).²¹⁾

$$\epsilon_m' = 1 - \frac{\omega_p^2 \tau^2}{1 + \omega^2 \tau^2} \quad (2),$$

where ω_p and τ is the plasma frequency and relaxation time, respectively. It is possible that the addition of copper atoms in gold particles as impurities decreases the relaxation time, resulting in an increase in ϵ_m' according to eq.(2). Eq.(2) also shows that ϵ_m' is higher, as the wavelength is shorter. The condition $\epsilon_m' = -2\epsilon_d$ is held at longer wavelengths

for the gold particles including copper atoms than pure gold particles. That is, the plasmon band of the gold particles including copper atoms is longer in wavelength than that of pure gold particles. Furthermore, it has been shown that the plasmon band due to the particles of Ag-Au alloy is located between the bands due to Au particles and Ag particles.²²⁾ As an analogy of Ag-Au alloy, it is expected that the plasmon band due to the particles of Au-Cu alloy is located between the bands due to Au particles and Cu particles. On the other hand, it is expected from the refractive index of Cu_2O ²³⁾ that the formation of Cu-O bonds in the glass increases the refractive index of the matrix glass. Since ϵ_m' decreases with an increase in wavelength, as mentioned above, the increase in ϵ_d leads to the shift of the plasmon band toward longer wavelength.

Third order nonlinear susceptibility $\chi^{(3)}$ was measured by a degenerated four-wave mixing method at room temperature. In this measurement, a frequency-doubled Q-switched Nd:YAG laser provided 44 ps pulses with an energy of about 16 MW/cm² and 8 ns pulses with an energy of 1.7 MW/cm² at a wavelength of 532 nm. Configuration of the measurement has been described elsewhere.²⁴⁾ The value of $\chi^{(3)}$ for 8 ns and 44 ps pulses was about 8×10^{-8} esu and 2×10^{-8} esu, respectively, in the co-implanted glass after heat-treatment.

V. Conclusions

The formation of ultrafine particles is controlled by the transport process of implanted atoms in matrix, although it tends to obey the thermodynamic stability. Ultrafine particles of copper-gold alloy were formed in silica glass by co-implantation of Au⁺ and Cu⁺ ions. It was deduced that competition between the collision process and precipitation process determines the resultant particle size. The peak wavelength of plasmon band in the co-implanted glasses was longer than that in Au⁺ ion implanted glass, after heat-treatment, probably due to the dissolution of Cu⁺ ions in silica matrix and the formation of Cu-Au alloy.

Acknowledgment:

This work has been performed under the approval of the Photon Factory Advisory Committee (Proposal No.95G027).

References

1. R.H.Haglund Jr., H.C.Mogul, R.A.Weeks and R.A.Zuhr, *J.Non-Cryst.Solids* **130**, 326 (1991).
2. K.Fukumi, A.Chayahara, K.Kadono, T.Sakaguchi, Y.Horino, M.Miya, K.Fujii, J.Hayakawa and M.Satou, *J. Appl. Phys.* **75**, 3075 (1994).
3. G. Ghislotti, B. Nielsen, P. Aoska-Kumar, K. G. Lynn, A. Gambhir, L. F. Di Mauro and C. E. Bottani, *J. Appl. Phys.* **79**, 8660 (1996).
4. Y. Horino, A. Chayahara, M. Kiuchi, K. Fujii, M. Satou and T. Takai, *Jpn. J. Appl. Phys.* **29**, 2680 (1990).
5. G. W. Arnold, *J. Appl. Phys.* **46**, 4466 (1975).
6. G. W. Arnold and J. A. Borders, *J. Appl. Phys.* **48**, 1488 (1977).
7. H. Hosono, H. Fukushima, Y. Abe, R. A. Weeks and R. A. Zuhr, *J. Non-Cryst. Solids*, **143**, 157 (1992).
8. H. Hosono, *Jpn. J. Appl. Phys.* **32**, 2892 (1993).
9. A. Perez, T. Treilleux, T. Capra and D. L. Griscom, *J. Mat. Res.* **2**, 910 (1987).
10. K. Fukumi, A. Chayahara, K. Kadono, H. Kageyama, T. Akai, N. Kitamura, M. Makihara, K. Fujii and J. Hayakawa, submitted to *J. Non-Cryst. Solids*.
11. K. Fukumi, A. Chayahara, J. Hayakawa and M. Satou, *Mat. Res. Soc. Symp. Proc.* **201**, 241 (1991).
12. Feng Yiping, *Acta Optica Sinica* **9**, 1039 (1987).
13. K. Fukumi, A. Chayahara, M. Makihara, K. Fujii, J. Hayakawa, M. Satou, *J. Am. Ceram. Soc.* **77**, 3019 (1994).
14. W. D. Kingery, H. K. Bowen and D. R. Uhlmann, *Introduction to Ceramics*, 2nd ed. (John Wiley & Sons, New York, 1976), Chap. 8, p.320.
15. C.Wert and C. Zener, *J. Appl. Phys.* **21**, 5 (1950)
16. K. Fukumi, A. Chayahara, M. Adachi, K. Kadono, T. Sakaguchi, M. Miya, Y. Horino, N. Kitamura, J.Hayakawa, K. Fujii and M.Satou, *Mat. Res. Soc. Symp. Proc.* **235**, 389 (1992)
17. K. Fukumi, H. Kageyama, K. Kadono, A. Chayahara, N. Kamijo, M.Makihara, K. Fujii, J. Hayakawa and M. Satou, submitted to *J. Mat. Res.*
18. A. Balerna, E. Bernieri, P. Picozzi, A. Reale, S. Santucci, E. Burattini and S. Mobilio,

- Phys. Rev. **B31**, 5958 (1985).
19. K. Fukumi, A. Chayahara, M. Makihara, K. Fujii, J. Hayakawa and M. Satou, *Appl. Phys. Lett.* **64**, 3410 (1994).
 20. K. Fukumi, H. Kageyama, K. Kadono, A. Chayahara, N. Kamijo, M. Makihara, K. Fujii, J. Hayakawa and M. Satou, *J. Mat. Res.* **10**, 2418 (1995).
 21. P.B.Johnson and R.W.Christy, *Phys.Rev.* **B6**, 4370 (1972).
 22. U.Kreibig and M.Volmer, *Optical Properties of Metal Clusters* (Springer, Berlin, 1995), Chap. 4.3, p.366.
 23. C.G.Ribbing and A.Roos, *Handbook of Optical Constants II*, edited by E.D.Palik (Academic Press, Orland, 1991), p.875.